The main green tea polyphenol epigallocatechin-3-gallate counteracts semen-mediated enhancement of HIV infection

Ilona Hauber[a,1], Heinrich Hohenberg[a], Barbara Holstermann[a], Werner Hunstein[b], and Joachim Hauber[a]

[a]Heinrich-Pette-Institute for Experimental Virology and Immunology, Martinistrasse 52, D-20251 Hamburg, Germany; and [b]Faculty of Medicine, University of Heidelberg, Schlosswolfsbrunnenweg 41, D-69118 Heidelberg, Germany

Edited by Peter K. Vogt, The Scripps Research Institute, La Jolla, CA, and approved April 2, 2009 (received for review November 20, 2008)

Peptide fragments, derived from prostatic acidic phosphatase, are secreted in large amounts into human semen and form amyloid fibrils. These fibrillar structures, termed semen-derived enhancer of virus infection (SEVI), capture HIV virions and direct them to target cells. Thus, SEVI appears to be an important infectivity factor of HIV during sexual transmission. Here, we are able to demonstrate that epigallocatechin-3-gallate (EGCG), the major active constituent of geen tea, targets SEVI for degradation. Furthermore, it is shown that EGCG inhibits SEVI activity and abrogates semen-mediated enhancement of HIV-1 infection in the absence of cellular toxicity. Therefore, EGCG appears to be a promising supplement to antiretroviral microbicides to reduce sexual transmission of HIV-1.

EGCG | microbicide | prostatic acidic phosphatase | SEVI | sexual transmission

On the global scale, the HIV-1 epidemic is primarily driven by heterosexual transmission, accounting for the vast majority of the currently 33 million people infected with this lethal pathogen (1). Because more than 96% of new infections occur in low- and middle-income countries, it is expected that the successful clinical development of antiretroviral drug-based microbicides may not only significantly slow sexual transmission of HIV-1 but may also provide a simple and affordable prevention method, particularly for application in resource-poor settings (reviewed in refs. 2 and 3).

During the process of identifying natural agents that interfere with HIV-1 replication, Münch et al. (4) recently identified a peptide fraction in human semen (SE) that consistently enhanced HIV-1 infection. The major enhancing activity was correlated with the presence of a peptide derived from the internal region of prostatic acidic phosphatase (PAP) (4), a protein that is produced by the prostatic gland and secreted in large quantities (1–2 mg/mL) into SE (5). Interestingly, the ability of this peptide, corresponding to PAP amino acid residues 248–286 (PAP248–286), to boost infectivity of a broad range of HIV-1 strains, including X4-, R5-, and dual-tropic isolates as well as group M and O strains, depended on its unexpected capacity to form β-sheet-rich amyloid fibrils (4). Although their exact mode of action is largely unknown, these fibrils, termed semen-derived enhancer of virus infection (SEVI), supposedly capture virions and attach them to the surface of target cells, thereby enhancing receptor-mediated virus–host cell fusion (discussed in ref. 6). Apparently, the positively charged SEVI decreases charge–charge repulsions that exist between virions and host cells (7). Thus, SE-derived, fibril-forming PAP fragments may strongly promote HIV transmission during sexual intercourse, particularly when low quantities of infectious virus are available to cross the mucosal barrier (reviewed in refs. 2 and 8). Moreover, the action of SEVI may be detrimental to the successful development of antiretroviral microbicides, a field of clinical research that currently faces various technical challenges (9). For these reasons, it is fair to assume that the inclusion of a SEVI inhibitor into an antiretroviral microbicide-based regimen may improve the potential of such a strategy to prevent sexual transmission of HIV-1.

Many highly diverse proteins are able to self-assemble into amyloid fibrils (10, 11), a process that is frequently associated with serious neurodegenerative disorders, such as Parkinson's disease and Alzheimer's disease (12, 13). A recent study was conducted to investigate whether small-molecule inhibitors can interfere with amyloid formation and, in particular, it has been demonstrated that the polyphenol epigallocatechin-3-gallate (EGCG) efficiently inhibits amyloid fibrillogenesis (14). EGCG is the major catechin in green tea and has been ascribed to exert various antitumorigenic, antioxidative, antibacterial, and antiviral effects (for reviews, see refs. 15–17). Because of its antifibrillogenic properties (14), we analyzed the potential of EGCG to target PAP248–286-derived fibrils and to interfere with SE-mediated enhancement of HIV-1 infection in the present study.

Results and Discussion

Effects of the Green Tea Catechin EGCG on PAP-Derived Amyloid Fibrils. The capacity of a synthetic PAP248–286 peptide to form amyloid fibrils was analyzed in the presence or absence of various concentrations of EGCG. Fibril formation of the freshly dissolved peptide (1 and 5 mg/mL in PBS) was initiated by agitation at 37 °C and monitored over time by Congo red staining, a standard method to detect amyloid fibrils (18). In agreement with previous data (4), fibril formation was easily observed at both peptide concentrations in absence of EGCG (Fig. 1*A*). Further inspection of the data revealed that EGCG interfered with fibrillogenesis in a dose-dependent fashion. The ratio of PAP248–286 to EGCG clearly affected the inhibitory capacity of EGCG in these experiments (Fig. 1*A*, compare *Upper* and *Lower*). High inhibitor levels (10 and 20 mM EGCG) completely abrogated the formation of fibrils at both inhibitor concentrations. Furthermore, when EGCG was present in the reaction at lower concentrations (i.e., 1 and 5 mM), newly formed fibrils were apparently degraded over time (Fig. 1*A*).

To analyze this effect further, we next exposed preformed PAP248–286 fibrils, which were generated in the absence of inhibitor, to various concentrations of EGCG. Again, the status of fibrillogenesis was determined over time by Congo red staining. As shown in Fig. 1*B*, SEVI (5 mg/mL) was highly stable over a time period of 48 h. Obviously, fibril formation even

Author contributions: I.H. and J.H. designed research; I.H., H.H., and B.H. performed research; W.H. contributed new reagents/analytic tools; I.H., H.H., and J.H. analyzed data; and I.H. and J.H. wrote the paper.

The authors declare no conflict of interest.

This article is a PNAS Direct Submission.

Freely available online through the PNAS open access option.

[1]To whom correspondence should be addressed. E-mail: ilona.hauber@hpi.uni-hamburg.de.

This article contains supporting information online at www.pnas.org/cgi/content/full/0811827106/DCSupplemental.

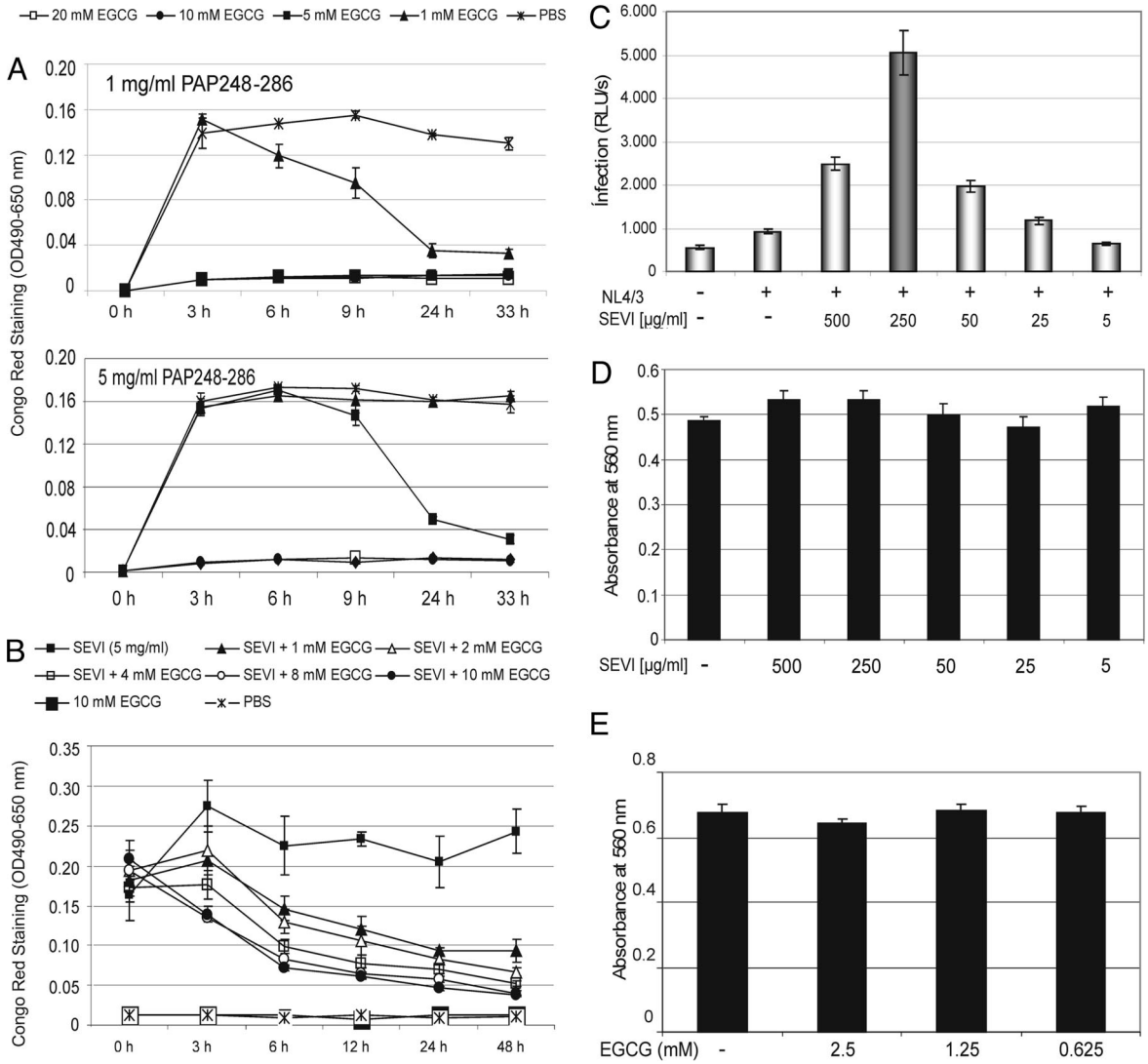

Fig. 1. EGCG targets synthetic PAP248–286-derived amyloid fibrils. (*A*) Amyloid fibrils were formed by agitation of the fresh PAP248–286 solutions (1 and 5 mg/mL) at 37 °C. Fibrillar aggregates were exposed to various concentrations of EGCG (□, 20 mM; ●, 10 mM; ■, 5 mM; and ▲, 1 mM) and detected by Congo red staining at the indicated time points. Addition of PBS alone (solvent for EGCG) served as negative control (×). (*B*) Preformed PAP248–286-derived fibrils (SEVI) were treated with increasing concentrations of EGCG (▲, 1 mM; △, 2 mM; □, 4 mM; ○, 8 mM; and ●, 10 mM) for 48 h and analyzed as before. Reactions containing EGCG alone (■, 10 mM) or PBS alone (×) served as controls. (*C*) HIV-1 particles (X4 strain NL4/3) were preincubated for 20 min with or without the indicated concentrations of SEVI. Subsequently, Jurkat 1G5 luciferase indicator cells were exposed to the respective virus/SEVI mixtures for 5 h. At 24 h after infection, RLU/s was determined. Error bars represent three independent experiments. (*D*) Cellular metabolic activity was tested in uninfected Jurkat 1G5 cells by alamarBlue assay after 5 h of exposure to the indicated concentrations of SEVI. (*E*) Viabilities of uninfected Jurkat 1G5 cells were determined after 5 h exposure to the indicated EGCG concentrations as before.

slightly increased within the initial 3 h of incubation. In sharp contrast, however, addition of EGCG to the preformed amyloid fibrils apparently triggered their degradation, which was again observed in a dose-dependent manner. As expected, control reactions, in which PBS only (solvent for EGCG) or EGCG only (10 mM) was analyzed, did not score in this experiment.

We next wanted to confirm that our SEVI samples are indeed able to promote HIV-1 infection. For this, various concentrations of SEVI were preincubated with HIV-1 strain NL4/3 particles for 20 min in a small volume. Subsequently, this virus/SEVI mixture was used to infect Jurkat 1G5 cells, which contain a stably integrated HIV-1 LTR-luciferase construct (19). Thus, infectability of these T cells can be quantified by measuring luciferase activity. At 24 h after infection, the respective analyses revealed the expected SEVI-mediated enhancement of HIV-1 infection, clearly reaching an optimum in these cells at a SEVI concentration of 250 μg/mL (Fig. 1*C*). The monitoring of cellular metabolic activity, as measured by alamarBlue assay, demonstrated that SEVI did not induce any detectable toxic effect on cellular viability in Jurkat 1G5 cells at these drug concentrations (Fig. 1*D*).

Despite the fact that the polyphenol EGCG is a major constituent of green tea (17), and is therefore generally recognized as safe for human consumption, we next analyzed potential undesired effects of EGCG on the viability of uninfected 1G5 cells. As shown in Fig. 1*E*, EGCG induced no deleterious effect in these cells, even at 2.5 mM, the highest concentration tested.

To more directly monitor the action of EGCG on SEVI, we next performed analyses at the ultrastructural level by using an ultrathin sectioning technique in combination with transmission electron microscopy. Solutions of SEVI or EGCG were encapsulated in capillary microtubes (200-μm diameter; Fig. 2), fixed

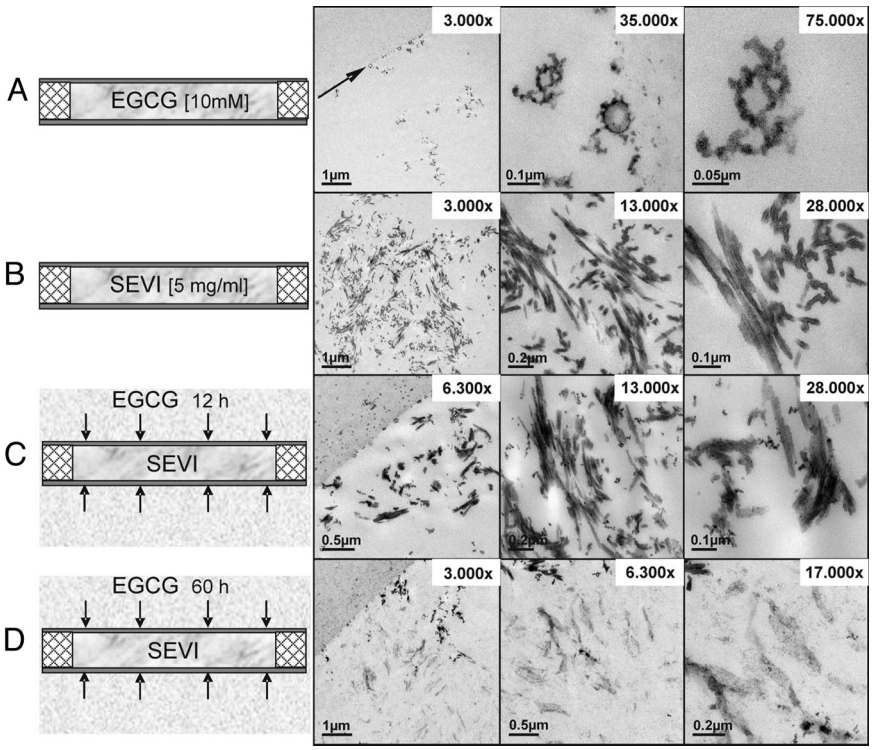

Fig. 2. Transmission electron microscopy analysis of EGCG-treated SEVI in a closed system. Corresponding images are arranged side by side. (*A*) Dissolved EGCG is shown inside the ultrathin sectioned microtubes and at different magnifications. The overview shows the interface between the tube wall (arrow) and the tube's lumen filled with EGCG. (Magnification: 3000×.) EGCG aggregates are organized in different patterns. (Magnifications: 35,000× and 75,000×.) (*B*) The SEVI solution shows a high density of SEVI-specific amyloid fibrils. (Magnification: 3,000×.) Because of the embedding angle, the fibrils often run out of the section plane. (Magnification: 28,000×.) Nevertheless, their length differs between 30 and 90 nm. (*C*) Appearance of SEVI after 12 h of incubation in EGCG. The small EGCG aggregates diffused from the outside through the porous wall into the lumen of the tube covering the surface of the fibrils. (Magnification: 6,300×.) (*D*) Degradation of the majority of SEVI after 60 h of incubation in 10 mM EGCG.

in situ, dehydrated, and embedded for subsequent staining of ultrathin sections and micrograph acquisition. As shown, a 10 mM solution of the polyphenol EGCG (molecular weight, 458.37) formed small aggregates, whereas significantly larger, typical fibrillary structures were observed in instances of SEVI at a concentration of 5 mg/mL (Fig. 1 *A* and *B*, respectively). To next visualize the action of EGCG on SEVI, sealed microtubes filled with dissolved SEVI fibrils were placed into a chamber filled with a solution of 10 mM EGCG and subsequently incubated over time, allowing the EGCG molecules to diffuse from the outside into the lumen of the tube. After incubation for 12 h and 60 h, the tubes were fixed, and samples were processed as before. The SEVI fibrils appeared to remain largely unaffected by EGCG after an incubation period of 12 h, although EGCG aggregates already covered the surface of the SEVI fibrils, which is particularly apparent at higher magnification (Fig. 2*C*). In sharp contrast, however, after incubation for 60 h, all SEVI-specific amyloid fibrils were extensively degraded (Fig. 2*D*), as visualized by the low contrast of the SEVI residues, directly confirming the data obtained before by Congo red staining. Thus, the combined experiments demonstrated that the polyphenol EGCG targets PAP248–286-derived amyloid fibrils.

The exact molecular mechanism of how EGCG degrades SEVI remains to be elucidated. However, recent experimental evidence indicates that EGCG inhibits amyloid formation of α-synuclein and amyloid-β by redirecting aggregation-prone molecules into unstructured oligomers, and EGCG also prevents the seeded aggregation of both polypeptides (14). It is therefore conceivable that EGCG may also exert similar inhibitory effects on the fibrillogenesis of SEVI-specific aggregates.

EGCG Inhibits the Activity of PAP248–286-Specific Amyloid Fibrils. It was earlier reported that EGCG interferes with HIV-1 replication (20, 21), and various antiviral mechanisms of EGCG were suggested, including inhibition of glycoprotein of M_r 120,000 (gp120)–CD4 interaction (22, 23) and direct blocking of envelope gp41-mediated membrane fusion (24). Therefore, we next wanted to analyze the potential antiviral effect of EGCG in the absence of SEVI. As shown in Fig. 3*A*, even at 2.5 mM, no significant antiviral EGCG effects on de novo infection were observed in HIV-1 NL4/3-infected Jurkat 1G5 cells. It was not surprising that no cellular toxicity was detectable in these cell cultures (Fig. 3*A*, red plot), particularly when the results of the cell viability tests performed before were also considered (Fig. 1 *D* and *E*).

Because EGCG apparently degrades SEVI, we next wanted to test whether EGCG indeed inhibits the infectivity-enhancing action of these amyloid fibrillary aggregates. We therefore again infected 1G5 cells with either the HIV-1 NL4/3 strain or the multiresistant BE4 isolate and monitored infectability by measuring luciferase activity as before. HIV-1 BE4 is a highly active antiretroviral therapy (HAART)-resistant virus with high-level resistance to multiple inhibitors of viral protease and reverse transcriptase (25). As described before, prior to infection the respective input viruses were preincubated for 20 min with SEVI (250 μg/mL) together with the concentrations of EGCG analyzed before to be nontoxic in these cells (Fig. 1*E*). These experiments confirmed again the infectivity-enhancing properties of SEVI and demonstrated that EGCG is indeed capable of effectively counteracting the activity of PAP248–286-derived fibrils in a dose-dependent fashion (Fig. 3*B*). In fact, at the highest concentration tested (2.5 mM), EGCG almost com-

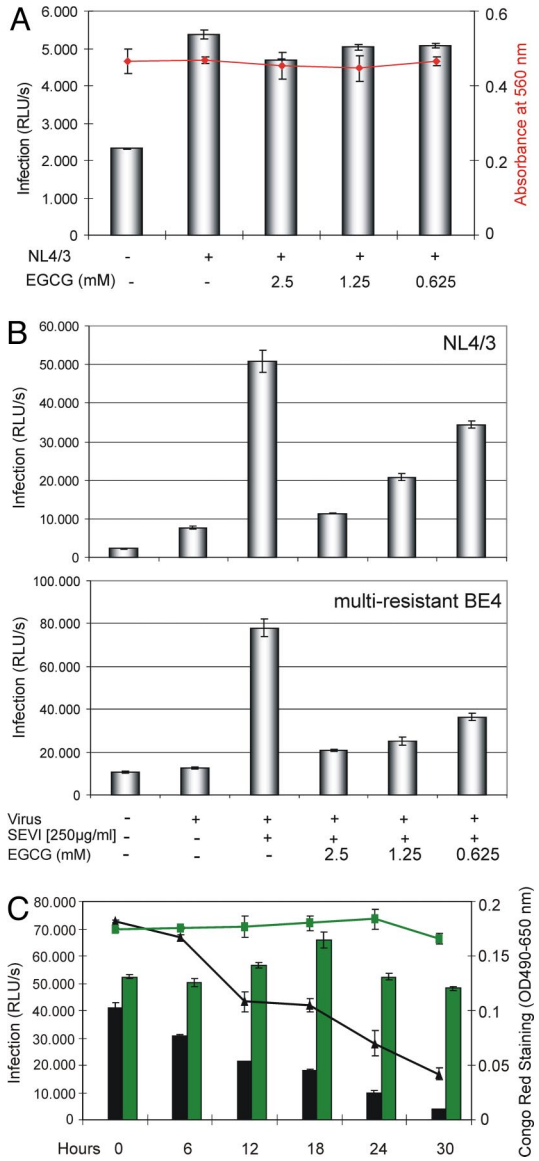

Fig. 3. The green tea catechin EGCG inhibits SEVI-mediated HIV infection. (*A*) Jurkat 1G5 cells were infected with HIV-1 NL4/3 in presence of the indicated concentrations of EGCG. The rate of infection was monitored by measuring the luciferase activity in the respective cell cultures (indicated as RLU/s; bars), and cell viabilities were determined by alamarBlue assay (red plot) 24 h after infection. (*B*) HIV-1 NL4/3 or the multiple antiretroviral drug-resistant virus isolate BE4 was preincubated for 20 min with 50 μg of SEVI and the indicated concentrations of EGCG. Using this mixture, 1G5 cells were subsequently infected for 5 h. At 24 h after infection, luciferase activity was measured as before. (*C*) Constant amounts (2.5 mM) of EGCG or GC were incubated together with SEVI (5 mg/mL) for the indicated time periods. The degradation of SEVI in each reaction was monitored by Congo red staining (EGCG: black plot; GC: green plot). Subsequently, equal aliquots of each reaction were used to infect 1G5 cells with HIV-1 NL4/3. The respective cultures were assayed as before (EGCG: black bars; GC: green bars).

pletely abrogated SEVI-specific boosting of virus infection. Moreover, this inhibitory effect was observed independent of the virus genotype or phenotype (i.e., strain NL4/3 vs. HAART-resistant BE4).

To further verify that the inhibitory activity of EGCG on HIV-1 infection in our experiments was primarily based on SEVI degradation, we now performed time course experiments in which the amount of SEVI and EGCG or gallocatechin (GC) was kept constant. GC is another catechin derivative in green tea (24) and served here as reaction control. As shown in Fig. 3*C*, increasing incubation times resulted in the gradual EGCG-mediated degradation of SEVI, as measured by Congo red staining in each reaction (Fig. 3*C*, black plot). In contrast, no SEVI degradation was observed when GC was analyzed (Fig. 3*C*, green plot). Importantly, a strictly linear correlation of the HIV-1 infectivity-boosting capacity of each sample with the amount of SEVI available in the respective EGCG-specific sample was observed (Fig. 3*C*, black bars). As expected, no inhibitory effect on virus infectivity was observed when GC was present (Fig. 3*C*, green bars).

In the next series of experiments, we used vesicular stomatitis virus glycoprotein-pseudotyped HIV-1 particles, which are able to bypass the otherwise strict requirement of the HIV-1 glycoproteins (gp120/gp41) for host cell infection. As shown in Fig. S1, SEVI also enhanced the infectivity of these pseudotyped virions, and this effect was again abrogated by EGCG.

To analyze the effect of EGCG on SEVI-mediated HIV-1 infection of primary cells, we infected peripheral blood mononuclear cells (PBMCs) with R5- and X4-tropic viruses in which the *nef* gene was replaced with a cDNA encoding firefly luciferase. Virus infectivity was analyzed essentially as before (Fig. S2). Furthermore, we also investigated SEVI and EGCG in conjunction with an R5-tropic or an R5X4 dual-tropic primary HIV-1 isolate in the cell line TZM-bl (Fig. S3). In contrast to the 1G5 cells used before, TZM-bl cells can be infected by both R5- and X4-tropic viruses, and similarly allow the quantification of HIV infection via an integrated, Tat-responsive luciferase reporter expression cassette (26). These experiments demonstrated that EGCG interfered with SEVI-mediated de novo infection of human PBMCs and also inhibited the enhancing properties of SEVI on the infectivity of primary HIV-1 isolates.

In sum, these data demonstrated that EGCG powerfully antagonizes the activity of SEVI by targeting and degrading these fibrillar structures.

EGCG Interferes with SE-Mediated Enhancement of HIV-1 Infection. To this point, we demonstrated that EGCG can efficiently suppress the action of SEVI that has been generated in vitro. However, any potential therapeutic application of EGCG (or of related compounds) depends on its ability to inactivate the infectivity-enhancing capacity of human SE. Thus, to more closely mirror the in vivo situation, we now included different human SE samples in our analyses.

It has been reported recently that addition of undiluted human SE might be toxic to cultured cells (4). Thus, we first investigated the infectivity-enhancing qualities of a serial dilution of a randomly selected human SE sample (SE#1). Infection of TZM-bl cells (26) with HIV-1 NL4/3 demonstrated that none of the SE#1 dilutions (1:2 to 1:32 in PBS/antibiotics) induced cellular toxicity (Fig. 4*A*, red plot), and that application of the 1:4 dilution in particular resulted in maximal infection of these cells (Fig. 4*A*). Subsequently, additional 1:4 dilutions of independent SE samples (SE#s 2–6) were compared side by side with SE#1 by using the same experimental setup (Fig. 4*B*). Inspection of the corresponding results indicated that individual human SE samples may vary considerably with respect to their HIV-1 infectivity-boosting properties (e.g., compare SE#s 4 and 5 in Fig. 4*B*). Nevertheless, the majority of these random samples significantly increased virus infection compared with the control experiment in which SE was omitted.

Then, the effect of EGCG on preventing SE-mediated enhancement of HIV-1 infection was tested on all SE samples essentially as described before. This series of experiments demonstrated that the SEVI inhibitor EGCG also efficiently abrogated the infectivity-enhancing properties of human SE in the absence of significant cellular toxicity (for SE#s 1 and 2, see Fig.

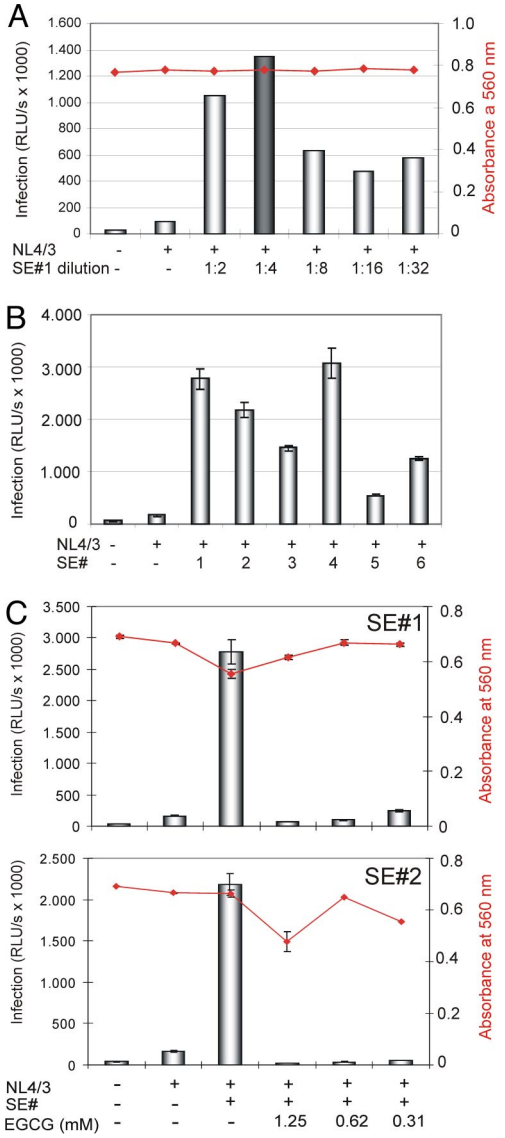

Fig. 4. EGCG abrogates SE-enhanced virus infection. (*A*) TZM-bl cells were infected with 50 ng of p24 antigen of replication-competent HIV-1 NL4/3 in the absence or presence of the indicated dilutions of a randomly selected human SE sample (SE#1). Noninfected cells and infected SE-untreated cells served as controls. Infectivity and cell viability (red plot) was determined essentially as before. (*B*) Six different SE samples (SE#s 1–6), diluted 1:4 in PBS, were analyzed in parallel as before. Experiments were performed in triplicate. (*C*) HIV-1 NL4/3 was exposed for 20 min to individual SE samples (SE#s 1 and 2) (1:4 dilution) in the presence or absence of the indicated EGCG concentrations. Subsequently, these mixtures were used for infection of TZM-bl cell cultures. Luciferase activity and cell viability (red plot) were determined at 24 h after infection as before. Error bars represent three independent experiments.

4*C*; for SE#s 3–6, see Fig. S4). In general, it appears that this inhibitory effect required lower drug concentrations, as in the experiments analyzing in vitro-generated SEVI (compare Figs. 3*B* and 4*C* and Fig. S4), and furthermore, some differences appear to exist between the various SE samples with respect to EGCG sensitivity (e.g., compare SEs 4 and 5 in Fig. S4), which may reflect differences in the amount of infectivity-enhancing fibrils that are present in the individual samples.

The combined data presented in this study suggest that the polyphenol EGCG targets PAP248–286-derived amyloid fibrils for degradation, thereby efficiently abrogating their HIV-1 infectivity-enhancing properties. Previous studies on the anti-HIV effects of EGCG focused on the potential for systemic application of this compound (20, 21). In contrast, our data argue in favor of the administration of EGCG (or functionally related drugs) as a topical agent, possibly as a supplement to antiretroviral microbicides. Their antiretroviral potency may thereby be improved because of EGCG-mediated compensation of the infectivity-boosting qualities of human SE. The fact that EGCG is very stable in acidic solution (27), a condition similar to the vaginal environment, further supports this notion.

The data presented in previous reports showing that EGCG inhibits HIV-1 by directly interacting with CD4 and/or HIV-1 Env (22–24) may provide an additional antiviral benefit with respect to the usage of EGCG as a component of future microbicides. In the present study, the pronounced inhibitory activity of EGCG on HIV-1 infectivity was mainly based on its ability to degrade SEVI. Nevertheless, at high drug concentrations, virus infectivity was in some experiments (e.g., Figs. S1 and S3) reduced to below that of the corresponding control experiment lacking SEVI. This may indeed reflect a direct effect of EGCG on the CD4 receptor and/or the viral glycoproteins.

Taken together, the polyphenol EGCG, a natural ingredient of green tea, may be a valuable and cost-efficient inhibitor of SE-mediated enhancement of virus infection, and hence of sexual transmission of HIV-1.

Materials and Methods

Reagents. The green tea catechins, EGCG and GC, were obtained from Sigma–Aldrich, and stock solutions of 100 mM or 50 mM, respectively, were prepared in PBS. Aliquots of various dilutions were stored at −20 °C.

Amyloid Fibril Formation by PAP248–286 and Photometric Detection. Synthetic peptides corresponding to PAP (European Molecular Biology Laboratory accession no. AAB60640) amino acid residues 248–286 (PAP248–286) were obtained from Davids Biotechnologie and Bachem. Lyophilized peptides were resuspended in PBS at a stock concentration of 10 mg/mL, and aliquots were stored at −20 °C. Fibril formation by the freshly dissolved peptide (1 or 5 mg/mL) was initiated by agitation at 37 °C and 1,200 rpm for 2–3 days (i.e., until the solution became turbid) by using an Eppendorf thermomixer. Formation of amyloid structures was routinely monitored by mixing 5-μL aliquots of the respective reaction batch with 100 μL of Congo red solution (20 μg/mL in PBS; Sigma). The solution was incubated for 10 min at ambient temperature and centrifuged for 5 min at 20,800 × *g* in an Eppendorf centrifuge 5417R. Supernatants were discarded, the pellets were dissolved in 100 μL of DMSO, and fibril formation was determined at $OD_{490-650}$ nm using an ELISA reader.

Treatment of SE. SE samples were donated by healthy volunteers, diluted with equal volumes of PBS containing 100 units/mL penicillin, 100 μg/mL streptomycin, and 50 μg/mL gentamycin (Gibco), and stored at −20 °C.

Analysis of Cellular Toxicity. Cell viability was analyzed by measuring cellular metabolic activity using the alamarBlue redox indicator (Serotec) in accordance with the manufacturer's protocol.

Cell Cultures and HIV Infection Experiments. Viruses were produced as described in the *SI Materials and Methods*. The suspension cell line 1G5 was cultured in RPMI medium 1640 containing 10% FCS (PanSystems) and antibiotics (penicillin and streptomycin). 1G5 cells are Jurkat derivatives containing a stably integrated HIV-LTR-firefly luciferase construct (19). Before infection, 50 ng of p24 antigen of the respective virus stock, 50 μg of PAP248–286-derived amyloid fibrils (SEVI), and various concentrations of EGCG, GC, or PBS (negative control) were incubated in a sterile reaction tube for 20 min using an Eppendorf thermomixer at 37 °C and 800 rpm. Thereafter, the respective mixtures were added to 10^6 1G5 cells and further incubated in a volume of 200 μL at 37 °C and 5% CO_2. Control experiments omitted the input virus, SEVI, or EGCG. After a 5-h incubation period, cells were washed once with PBS, and the cell pellet was resuspended in 1 mL of medium and further cultured in 24-well plates. At 24 h after infection, cell cultures were divided. One half was used to analyze cell viability. The cells of the remaining half were lysed in 100 μL of passive lysis buffer, and luciferase activity was measured as relative light units per second (RLU/s) according to the manufacturer's protocol (Promega).

Primary HIV-1 isolates were analyzed in 4 × 10^5 TZM-bl cells essentially as described before. The TZM-bl cell line allows the quantification of HIV infec-

tion either via an integrated Tat-responsive β-galactosidase or firefly luciferase reporter expression cassette (26). Likewise, TZM-bl cells were also used to investigate the infectivity-enhancing properties of independent human SE samples. For this, 200 μL of a 1:4 dilution of independent SE samples in PBS was mixed with 50 ng of p24 antigen of HIV-1 NL4/3 together with various concentrations of EGCG (total volume, 300 μL) and incubated in an Eppendorf thermomixer at 37 °C and 800 rpm for 20 min. Thereafter, 30 μL of the mixtures was added to 10^4 TZM-bl cells in a volume of 100 μL and incubated at 37 °C for 3 h, washed once, and further cultured in 200 μL of DMEM (10% FCS, penicillin, and streptomycin) in a 96-well, flat-bottom plate. At 24 h after infection, virus infectivity and cell viability were determined. As before, controls omitting input virus, SE, or EGCG were also included in the experimental design.

Ficoll-isolated PBMCs from healthy donors were treated with ammonium chloride, pH 7.4, for 20 min on ice to lyse erythrocytes, washed twice with PBS, and incubated in RPMI with 5% FCS, penicillin, and streptomycin. Subsequently, PBMCs were activated by using CD3/CD28 Dynabeads (Invitrogen) according to the manufacturer's protocol. At 24 h after stimulation, 2×10^6 PBMCs were pelleted, resuspended, and incubated in a volume of 250 μL together with input virus (50 ng of p24 antigen), 50 μg of SEVI, and various concentrations of EGCG. As before, prior to infection input virus, SEVI and EGCG were preincubated in an Eppendorf thermomixer for 20 min at 37 °C and 800 rpm. Controls omitting input virus, SEVI, or EGCG were included in the experimental design. After 5 h of incubation, cells were washed with PBS and further cultured in 1 mL of medium in a 24-well plate for another 24 h. Thereafter, one half of the PBMCs were analyzed for cell viability, and the other half of the cells were lysed with passive lysis buffer for subsequent luciferase analysis as described before.

Electron Microscopy. For ultrastructural analysis of the dissolved components in the transmission electron microscope (TEM), the solutions of SEVI (5 mg/mL) and EGCG (10 mM) were encapsulated in capillary microtubes and processed for ultrathin sectioning technique as already described in principle and detail (28). The microtubes (200-μm diameter) were filled with the solutions by capillary attraction and mechanically sealed at both ends by a scalpel. The dissolved components within the tubes were fixed in situ from the outside through the highly porous tube walls (molecular weight cut-off: 10 kDa) by successive immersion into 2.5% glutaraldehyde, 1% uranyl acetate, and 1% OsO_4 in PBS for 30 min each, followed by dehydration in a graded series of ethanol. For ultrathin sectioning, the microtubes were embedded in EPON (Carl Roth) resin. Sections were counterstained with 2% uranyl acetate and lead citrate. Electron micrographs were acquired with a Philips CM 120 TEM at 80 kV using a Gatan Multiscan 794 Camera.

To illustrate the action of EGCG on SEVI, sealed microtubes filled with dissolved SEVI were incubated into an EGCG solution. After defined reaction times, the tubes were fixed and processed as described above.

ACKNOWLEDGMENTS. We thank Andrea Bunk and Niklas Beschorner for excellent technical assistance and members of the laboratory for sample donation. We are indebted to Mel Smith for critical comments on the manuscript. The following reagents were obtained through the National Institutes of Health (NIH) AIDS Research and Reference Reagent Program, Division of AIDS, National Institute of Allergy and Infectious Diseases, NIH: 1G5 cells, catalogue no. 1819, from Drs. Agiular-Cordova and Stewart N. Davis; TZM-bl cells, catalogue no. 8129, from Dr. John C. Kappes, Dr. Xiaoyun Wu and Tranzyme; the primary HIV-1 R5 isolate 92TH026, catalogue no. 1693 from the Joint United Nations Programme on HIV/AIDS (UNAIDS) Network for HIV Isolation and Characterization; the primary HIV-1 R5X4 isolate 93BR020, catalogue no. 2329, from Drs. Beatrice Hahn and Feng Gao, and the UNAIDS Network for HIV Isolation and Characterization. We also thank Dr. Michael Schindler (Heinrich-Pette-Institute) for pBRNL4/3–92TH014Luc DNA. The Heinrich-Pette-Institute is a member of the Leibniz Gemeinschaft (WGL) and is supported by the Free and Hanseatic City of Hamburg and the Federal Ministry of Health.

1. UNAIDS (2007) AIDS epidemic update. Available at http://data.unaids.org/pub/EPISlides/2007/071118_epi_regional%20factsheet_en.pdf. Accessed November 17, 2008.
2. Shattock RJ, Moore JP (2003) Inhibiting sexual transmission of HIV-1 infection. *Nat Rev Microbiol* 1:25–34.
3. Klasse PJ, Shattock R, Moore JP (2008) Antiretroviral drug-based microbicides to prevent HIV-1 sexual transmission. *Annu Rev Med* 59:455–471.
4. Münch J, et al. (2007) Semen-derived amyloid fibrils drastically enhance HIV infection. *Cell* 131:1059–1071.
5. Rönnberg L, Vihko P, Sajanti E, Vihko R (1981) Clomiphene citrate administration to normogonadotropic subfertile men: Blood hormone changes and activation of acid phosphatase in seminal fluid. *Int J Androl* 4:372–378.
6. Roan NR, Greene WC (2007) A seminal finding for understanding HIV transmission. *Cell* 131:1044–1046.
7. Roan NR, et al. (2009) The cationic properties of SEVI underlie its ability to enhance HIV infection. *J Virol* 83:73–80.
8. Haase AT (2005) Perils at mucosal front lines for HIV and SIV and their hosts. *Nat Rev Immunol* 5:783–792.
9. Grant RM, et al. (2008) Whither or wither microbicides? *Science* 321:532–534.
10. Dobson CM (2003) Protein folding and misfolding. *Nature* 426:884–890.
11. Rochet JC, Lansbury PT, Jr (2000) Amyloid fibrillogenesis: Themes and variations. *Curr Opin Struct Biol* 10:60–68.
12. Taylor JP, Hardy J, Fischbeck KH (2002) Toxic proteins in neurodegenerative disease. *Science* 296:1991–1995.
13. Sacchettini JC, Kelly JW (2002) Therapeutic strategies for human amyloid diseases. *Nat Rev Drug Discov* 1:267–275.
14. Ehrnhoefer DE, et al. (2008) EGCG redirects amyloidogenic polypeptides into unstructured, off-pathway oligomers. *Nat Struct Mol Biol* 15:558–566.
15. Yang CS, Maliakal P, Meng X (2002) Inhibition of carcinogenesis by tea. *Annu Rev Pharmacol Toxicol* 42:25–54.
16. Nance CL, Shearer WT (2003) Is green tea good for HIV-1 infection? *J Allergy Clin Immunol* 112:851–853.
17. Cabrera C, Artacho R, Gimenez R (2006) Beneficial effects of green tea–a review. *J Am Coll Nutr* 25:79–99.
18. Frid P, Anisimov SV, Popovic N (2007) Congo red and protein aggregation in neurodegenerative diseases. *Brain Res Rev* 53:135–160.
19. Aguilar-Cordova E, Chinen J, Donehower L, Lewis DE, Belmont JW (1994) A sensitive reporter cell line for HIV-1 tat activity, HIV-1 inhibitors, and T cell activation effects. *AIDS Res Hum Retroviruses* 10:295–301.
20. Fassina G, et al. (2002) Polyphenolic antioxidant (-)-epigallocatechin-3-gallate from green tea as a candidate anti-HIV agent. *AIDS* 16:939–941.
21. Yamaguchi K, Honda M, Ikigai H, Hara Y, Shimamura T (2002) Inhibitory effects of (-)-epigallocatechin gallate on the life cycle of human immunodeficiency virus type 1 (HIV-1). *Antiviral Res* 53:19–34.
22. Kawai K, et al. (2003) Epigallocatechin gallate, the main component of tea polyphenol, binds to CD4 and interferes with gp120 binding. *J Allergy Clin Immunol* 112:951–957.
23. Williamson MP, McCormick TG, Nance CL, Shearer WT (2006) Epigallocatechin gallate, the main polyphenol in green tea, binds to the T-cell receptor, CD4: Potential for HIV-1 therapy. *J Allergy Clin Immunol* 118:1369–1374.
24. Liu S, et al. (2005) Theaflavin derivatives in black tea and catechin derivatives in green tea inhibit HIV-1 entry by targeting gp41. *Biochim Biophys Acta* 1723:270–281.
25. Hauber I, et al. (2005) Identification of cellular deoxyhypusine synthase as a novel target for antiretroviral therapy. *J Clin Invest* 115:76–85.
26. Wei X, et al. (2002) Emergence of resistant human immunodeficiency virus type 1 in patients receiving fusion inhibitor (T-20) monotherapy. *Antimicrob Agents Chemother* 46:1896–1905.
27. Zhu QY, Zhang A, Tsang D, Huang Y, Chen ZY (2008) Stability of green tea catechins. *J Agric Food Chem* 45:4624–4628.
28. Hohenberg H, Mannweiler K, Muller M (1994) High-pressure freezing of cell suspensions in cellulose capillary tubes. *J Microsc* 175:34–43.